Sensor and Simulation Notes

Note 422

January 1998

Estimating the Optimum Aperture for Maximizing Prompt Aperture Efficiency in an IRA

J. S. Tyo
Air Force Research Laboratory/DEHP
Kirtland AFB, NM 87117

ABSTRACT

This note provides a straightforward analytic means for approximating the ideal aperture for a flat-plate transmission-line feed for an IRA. Previously, the ideal aperture was obtained using numerical methods that are inflexible, and hence not suitable for use in designing systems. The method introduced here provides a means for rapidly estimating the ideal aperture so that any modifications for a realistic system can easily be made without requiring costly recomputing of the aperture. The resulting aperture efficiency of an antenna with an aperture designed using the approximate methods described here is within 0.5% of the efficiency of an IRA with the ideal aperture.

I. Introduction

In a recent note [1], the concept of prompt aperture efficiency for impulse radiating antennas (IRAs) was introduced. For focused aperture systems, the radiated field on boresight a distance r in the far-field limit is given by [2]

$$\bar{\mathbf{E}}_{rad}(r,t)=\frac{1}{2\pi rc}\frac{d}{dt}\iint_A \bar{\mathbf{E}}(x,y,t-r/c)dxdy\,, \tag{1}$$

where $c=1/\sqrt{\mu\varepsilon}$ is the speed of light in the medium, and the surface integral of the field is taken over a planar aperture defined by area A. By taking the ratio between the prompt field radiated from a particular IRA in accordance with (1) to the prompt field radiated by a test antenna, which has the same aperture uniformly illuminated, the aperture efficiency is [1]

$$\eta_A=\frac{A}{{V_{in}}^2}\frac{Z_{lin}}{Z_{med}}\langle E_y\rangle^2\,,\ \text{with}\ \langle E_y\rangle=\frac{1}{A}\iint_A E_y(x,y)dxdy\,. \tag{2}$$

In (2), Z_{lin} and Z_{med} are the impedance of the transmission-line feed structure of the IRA and the wave impedance of the medium, respectively.

In [1], the optimum aperture, i.e. the aperture that maximizes (2) for any particular feed structure, was determined to be bounded by a contour of constant E_y. The particular contour that yields the optimum aperture is that on which

$$E_y=\frac{\langle E_y\rangle}{2}\,. \tag{3}$$

Previously, numerical methods were used to determine the contour that satisfied (3) for various flat plate feed geometries. While effective, these methods are cumbersome and require reevaluation of the entire problem to determine the ideal aperture for a modified antenna structure. In this investigation, analytic techniques are given that can yield a close approximation to the ideal aperture for an IRA fed by a parallel, flat plate transmission line.

II. Analysis of the Limits

Knowing the field everywhere within a given contour is not enough to be able to determine if (3) is satisfied. The integral in (2) that gives $\langle E_y\rangle$ must also be evaluated, and in many feed structures of interest, this can be rather difficult. As discussed below, the field distribution on conical flat-plate feeds is given by the Jacobian Zeta function of the complex potential in two dimensions [3], and the resulting field distribution is difficult to deal with in the integral of (2).

In the previous study [1], the limiting cases for parallel plate transmission lines depicted in figs. 1 and 2, i.e. $Z\to 0$ $(a>>b$, where a is the plate width and b is the plate separation$)$ and

$Z \to \infty$ $(b >> a)$, were examined to determine asymptotic characteristics of the ideal aperture. Here, those analyses are spelled out more completely, and observations are made that yield insight into the more complex (and more practical) problem involving flat plates of finite width.

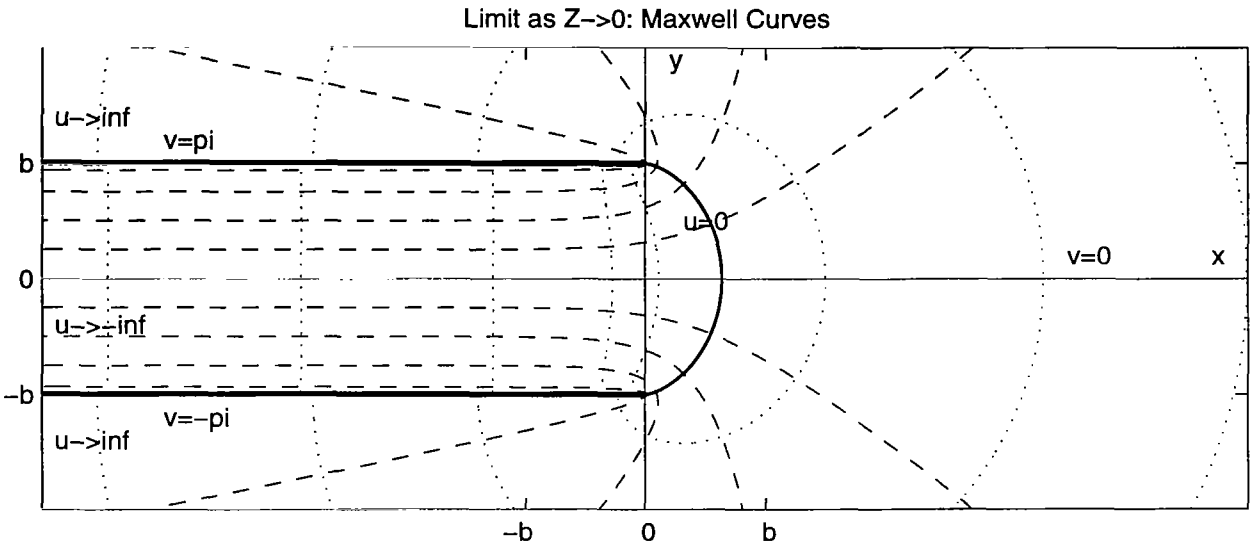

Figure 1: The limiting case of a parallel-plate transmission line as the impedance gets very small. The conformal mapping is known as "Maxwell Curves" and is given in (4). The ideal aperture includes all of the area between the plates (extending to -∞) as well as the area outside the plates bounded by the solid line labeled u=0. The y-component of the field on this contour is exactly half of the value of the field between the plates as x→-∞.

A. Limit of Very Close Plates $(Z \to 0)$

As the width of the plates becomes much greater than their separation, the structure (at least close to the edge) begins to look like a pair of semi-infinite plates that end abruptly at some location taken as $x=0$. The conformal map that gives the potential distribution on a pair of semi-infinite plates separated by a distance b is given in [3, E5] as the Maxwell curves:

$$z=\frac{b}{\pi}\left(w+1+e^{w}\right), \tag{4}$$

where $z=x+iy$ is the complex coordinate and $w=u+iv$ is the complex potential. With the form given by (4), the imaginary part of the complex potential, which varies as $-\pi \le v \le \pi$, is taken as the electric potential (i.e. $\bar{\mathbf{E}}=-\nabla v$), and the real part of the complex potential, which varies as $-\infty < u < \infty$, gives the stream function (field lines) [4]. It is clear that the ideal aperture will include most of (if not all of) the area between the plates, and possibly a portion of the area outside the plates. Given the semi-infinite nature of the structure, $\langle E_y \rangle$ can be determined by inspection for any aperture that includes the area between the electrodes as

$$\langle E_y \rangle = -\frac{\pi}{b}, \tag{5}$$

so the contour of interest is the one on which $E_y=-\pi/(2b)$. The complex field is determined from (4) (with v taken as the electric potential) as

$$\begin{aligned} E_c &= E_y + iE_x = -\frac{dw}{dz}, \\ E_y &= \mathrm{Re}\left[-\left(\frac{dz}{dw}\right)^{-1}\right] = -\frac{\pi}{b}\frac{1+e^{u}\cos v}{1+2e^{u}\cos v+e^{2u}} \end{aligned} \tag{6}$$

Setting the right side of (6) equal to $\pi/(2b)$ yields $u=0$ as the contour of constant E_y of interest. This contour is depicted in fig. 1, and is parameterized as a function of v as

$$x=\frac{b}{\pi}(1+\cos v),\ y=\frac{b}{\pi}(v+\sin v); \qquad -\pi \le v \le \pi. \tag{7}$$

There are two important properties of this contour that should be noted now:

1) The field at the point where the contour intercepts the plane of symmetry is exactly *half* of the value at the center of the aperture (i.e. $x \to -\infty$)

2) The contour for the optimum aperture lies *on a field line* (a line of constant u). Which field line? The *one* that leaves from the singularity.

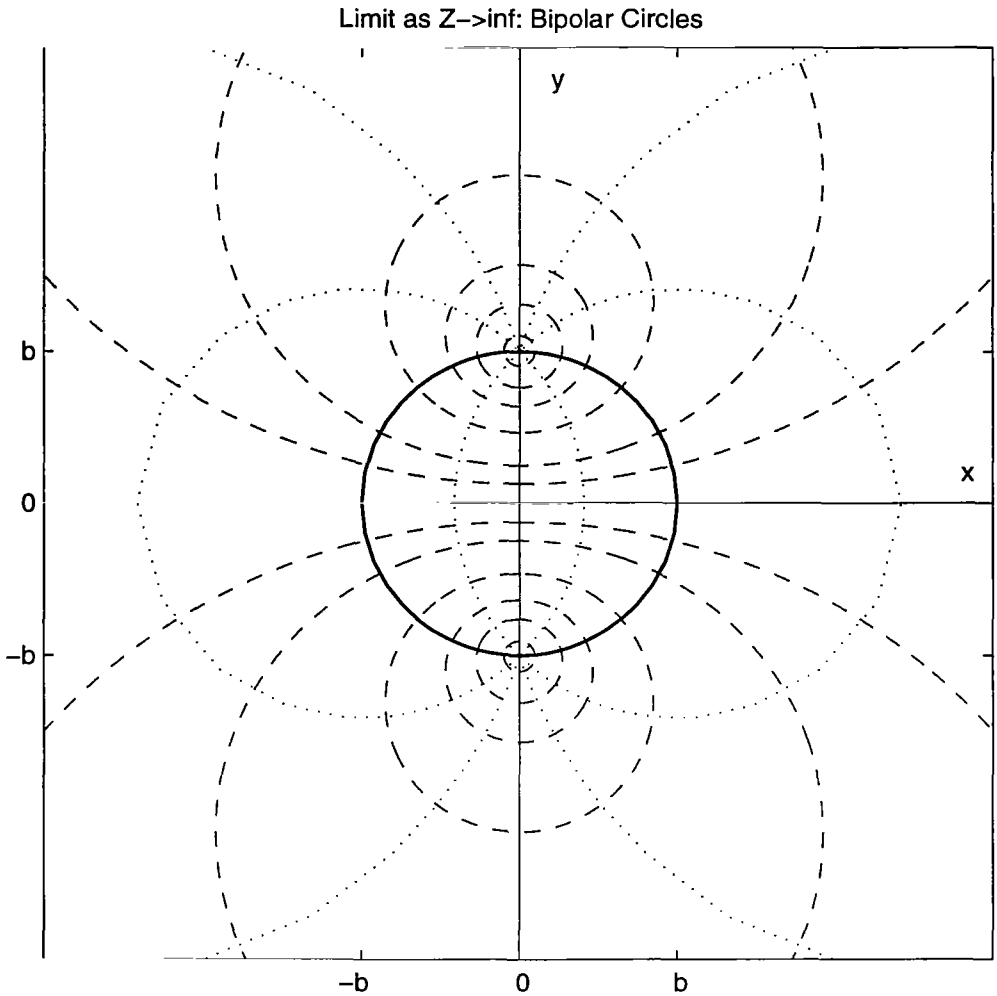

Figure 2: The limit of a high-impedance transmission line. As the plates get narrower and narrower, they begin to look like thin wires separated by b. The conformal transformation is given in (8) and is known as "Bipolar Circles." In this case, the ideal aperture lies on the circle of symmetry, shown solid here, where the y-component of the field is exactly half of the value at the origin.

B. Limit of Very Narrow Plates $(Z \to \infty)$

As the width of the plates gets to be much smaller than their separation, they begin to look like a pair of thin wires separated by distance b. The conformal map that gives the potential distribution for this case is given in [3, E4] as

$$z = \frac{ib\left(e^{w}+1\right)}{e^{w}-1}. \tag{8}$$

With the transformation in (8), the real part of the complex potential, which varies as $-\infty < u < \infty$, gives the electric potential, and the imaginary part of the complex potential, which

varies as $-\pi \le v \le \pi$, gives the stream function. Using (8) and taking advantage of the self-reciprocal properties of the aperture [5], a curve that satisfies (3) can be found by inspection.

The aperture for the two wire case depicted in fig. 2 is an example of a self-reciprocal aperture, i.e. an aperture that is unchanged by reciprocation of all points through a circle of symmetry. For the case of interest, this circle is centered at the origin and has radius b. It is shown in [5] that the average field inside such an aperture is identically equal to the value of the field at the center of the aperture. The relative electric field is (as a function of the complex *potential*, note that now u is taken as the electric potential)

$$E_c = E_x + iE_y = \frac{dw}{dz} = \frac{i}{b}(\cosh w - 1). \tag{9}$$

At the origin $(x=0, y=0; u=0, v=\pi)$, (9) gives $E_c = -i(2/b)$. On the circle of symmetry $(v=\pi/2, v=3\pi/2)$, (9) gives $E_c = -i(1/b)$. It is therefore clear that (3) is satisfied when the aperture is taken as the circle of symmetry. Again, there are two important properties of this contour that should be noted now:

1) The field at the point where the contour intercepts the plane of symmetry is exactly *half* of the value at the center of the aperture.

2) The contour for the optimum aperture lies *on a field line* (a line of constant u). Which field line? The one that leaves *horizontally* from the singularity..

Apparently, the ideal aperture for the two limiting cases is bounded by a field line that leaves the singularity in the horizontal direction and has a constant value of E_y equal to half the value of the field at the center of the aperture. It is possible that these observations might provide insight to the selection of the ideal aperture for an arbitrary parallel-plate transmission-line feed.

III. Arbitrary Parallel-Plate Feed

Given the results of the previous section, one might be inclined to present the hypothesis, "The ideal aperture, as defined by (3), for an arbitrary parallel plate transmission-line feed structure is bounded by the field line that leaves (horizontally) from the singularity at the edge of the plate." In this section, this hypothesis is examined, and shown to be incorrect. However, it is also shown that the field line that leaves horizontally from the singularity is in fact a good approximation to the boundary of the ideal aperture.

The conformal transformation that gives the field distribution on a parallel-plate transmission line has been investigated in many places [6,7]. While this transformation does not give the exact potential distribution for TEM horns with large flare angles [8], it does work well for small-angle TEM horns like those typically used for the feed structure in lens IRAs [9,10]. The transformation used here is given in [3, J6] as

$$\bar{z} = x - iy = \frac{2K(m)b}{\pi} Z(w + iK(1-m)|m) + ib \tag{10}$$

where $K(m)$ is the complete elliptic integral of the first kind evaluated at the parameter m [11, ch. 17] and $Z(w|m)$ is the Jacobi zeta function [11, ch. 17]. The parameter m is set by the specific impedance of the horn [6,7]. Note that this transformation is somewhat different in form from that used in [7] and [9]. As shown in [3], the imaginary part of the complex potential, which varies as $-K(1-m) \le v \le K(1-m)$, gives the electric potential and the real part of the complex potential, which varies as $-K(m) \le u \le K(m)$, gives the stream function. The contours that define the plates are at $v = \pm K(1-m)$.

The first order of business is to determine the value of u at the singularity. Once that value is determined, that particular field line can be evaluated to determine if it satisfies (3). The metric coefficient for a conformal transformation in two-dimensions gives the differential area element in terms of the complex potential, i.e. $dA = g_{11} du dv$. The singularity is located at the point where the metric coefficient is equal to zero (i.e. a change in either u or v produces no change in the complex coordinate z). We already know that singularities lie at the edges of the flat plates. Furthermore, by symmetry, finding the location of one singularity gives the location of the other three. On the top electrode $(v = K(1-m))$, the metric coefficient given in [3] simplifies to

$$g_{11} = \left(\frac{2K(m)b}{\pi}\right)^2 \left(\mathrm{dn}^2(u|m) - \frac{E(m)}{K(m)}\right)^2, \tag{11}$$

where $\mathrm{dn}^2(u|m)$ is a Jacobi elliptic function [11, ch. 16]. Equation (11) is equal to zero when

$$\begin{aligned} \mathrm{dn}^2(u \mid m) &= \frac{E(m)}{K(m)}, \\ u = u_0 &= F(\phi_0 \mid m) \\ \sin\phi_0 = \mathrm{sn}(u \mid m) &= \sqrt{\frac{1}{m}\left(1 - \frac{E(m)}{K(m)}\right)} \end{aligned}, \tag{12}$$

where $F(\phi_0|m)$ is the incomplete elliptic integral of the first kind [11, ch. 17]. Note that (12) is in agreement with [6] as to the location of the singularity.

The next step in validating the hypothesis given above is to evaluate E_y on the contour of constant u given in (12). For the transformation given in (10), E_y is given by the real part of dw/dz. Using the definition of the Jacobian Zeta function [7,11] and the relation for the derivative of the incomplete elliptic integral of the second kind [11, 16.26.3], the complex (relative) field is found to be

$$E_y = \mathrm{Re}\frac{dw}{dz} = \mathrm{Re}\left(\left(\frac{dz}{dw}\right)^{-1}\right) = \mathrm{Re}\left[\frac{\pi}{2K(m)b}\left(\mathrm{dn}^2(w + iK(1-m)|m) - \frac{E(m)}{K(m)}\right)^{-1}\right]. \tag{13}$$

Unfortunately, it can be shown that $dE_y(u_0+iv)/dv \neq 0$ for at least one value of v for $0<m<1$. This implies that the ideal aperture *cannot* lie on a field line, since the ideal aperture *must* leave the electrode horizontally from the singularity (to ensure finite E_y) and since *only* the field line given by (12) leaves the electrode horizontally from the singularity.

IV. Use of Field Line as Approximation to Ideal Aperture

Now that we know that the optimum aperture for an arbitrary flat plate feed structure is not given by the field line that leaves horizontally from the singularity, we should determine how close this field line comes to approximating the ideal aperture. As is shown in this section, the aperture defined by the field line in question is a *good* approximation to the ideal aperture for flat plate feed structures.

A. Magnitude of the Field on the Plane of Symmetry

As shown above for the limiting cases, the magnitude of the y-component of the field on the ideal aperture at the plane of symmetry is exactly *half* of the y-component of the field at the origin. In this section, we compute the corresponding ratio for an arbitrary flat-plate feed and show that it asymptotes to ½ on both ends (low and high impedance).

Due to symmetry constraints, the field on the plane of symmetry is y-directed only. Evaluating (13) at the origin $(x=0, y=0; u=K(m), v=0)$ yields

$$E_y(K+i0) = -\frac{\pi}{2bE}, \tag{14}$$

and evaluating (13) at $u=u_0, v=0$ yields

$$E_y(u_0+i0) = \frac{\pi}{2Kb}\left(\frac{1-E/K}{(E/K)^2-2(E/K)+m_1}\right), \tag{15}$$

where the parameter of the complete elliptic integrals K and E has been suppressed in (14) and (15) and $m_1 = 1-m$. The ratio of (14) and (15) is plotted in fig. 3. Using expansions for K and E/K [11], the ratio can be shown to asymptote to ½ for m→0 and for m→1.

B. Location of the Intercept of the Field Line with the Plane of Symmetry

One of the important parameters calculated in [1] was the additional width of the ideal aperture as a function of aspect ratio. An empirical function was fit to the data that fit reasonably well for low impedances (i.e. $Z<200\Omega$). Here the intercept of the field line in question with the plane of symmetry is calculated and compared to the numerical results obtained previously.

The x and y coordinates for a particular u and v can be obtained from (10), but they are given directly in [3]. The quantity that we are interested in computing is

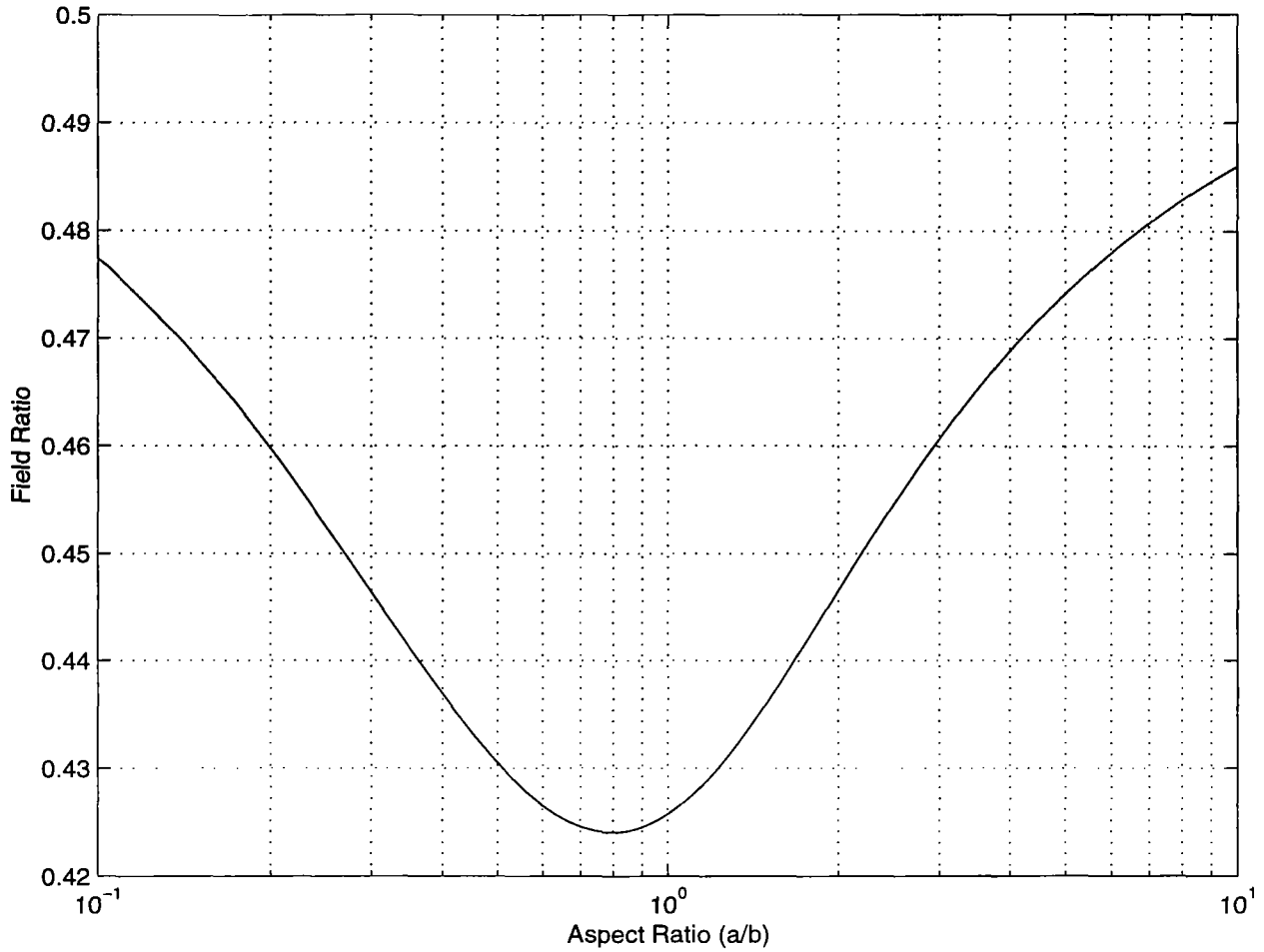

Figure 3: The ratio between the values of the field at the intercept of the field line with the plane of symmetry and at the origin. It was shown above and in [1] that for the limiting cases, this ratio should be ½. It is clear from the above plot that the limits as a/b→0 and as a/b→∞. Note that the ratio is furthest from ½ as values of a/b on the order just less that 1. This is the area where the field line makes the *worst* approximation to the ideal aperture, but as shown below, the fit is still quite good.

$(x_0 - a)/b$, where x_0 is the location of the intercept and a is the width of the plate as given in other sources as a function of plate separation and m [6,7]. The value of a is

$$a = \mathrm{Re}[\bar{z}(u_0 + iK(m_1))] = \frac{2K(m)}{\pi} Z(u_0 \mid m), \tag{16}$$

and the location of the intercept is

$$x_0 = \mathrm{Re}[\bar{z}(u_0 + i0)] = \frac{2K(m)}{\pi}\left\{ Z(u_0 \mid m) + \frac{m}{1 - \mathrm{dn}^2(u_0 \mid m)} \mathrm{sn}(u_0 \mid m)\mathrm{cn}(u_0 \mid m)\mathrm{dn}(u_0 \mid m) \right\}, \tag{17}$$

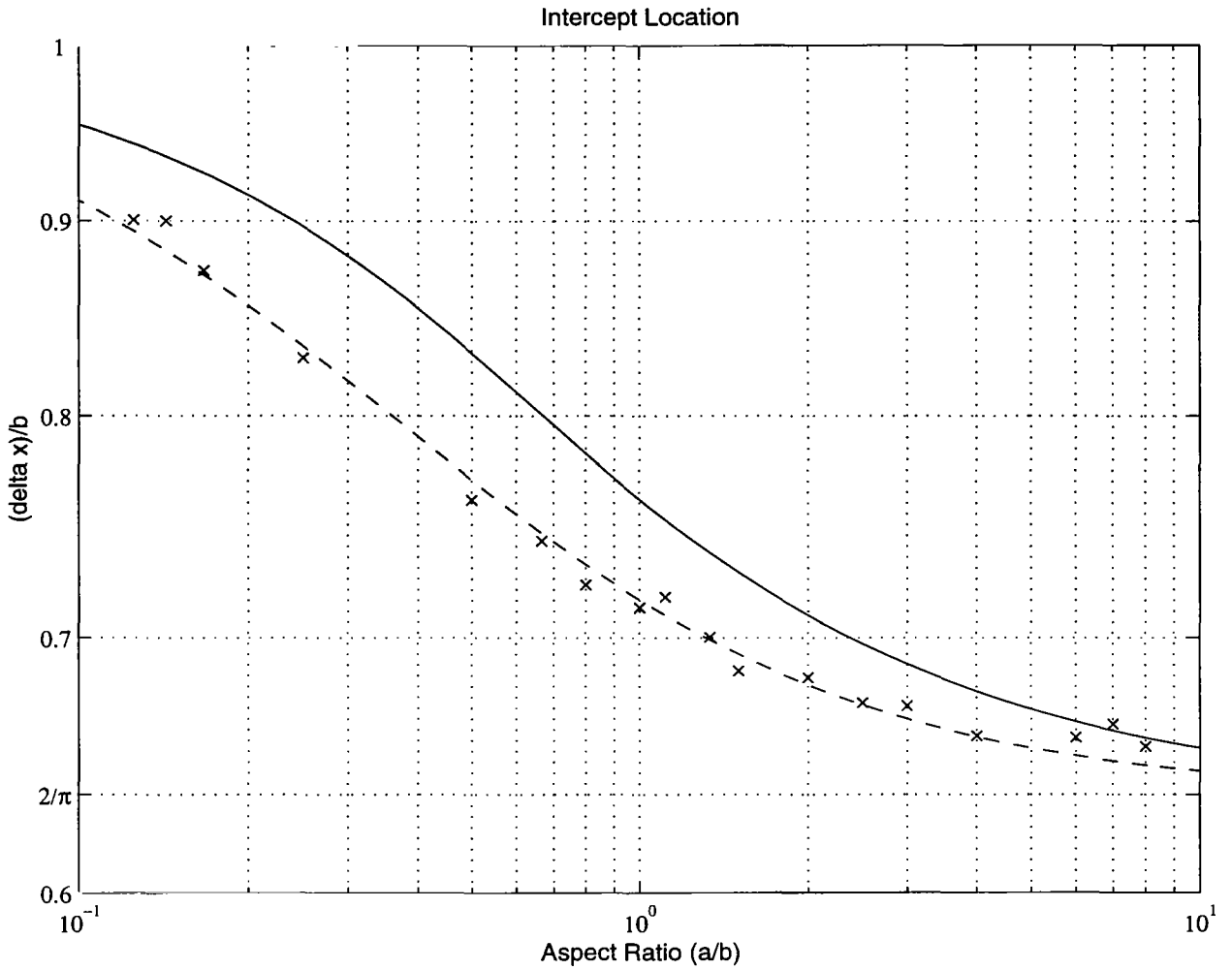

Figure 4: The extra width due to the aperture defined by the field line in question compared to the computed (and fit) data for the ideal aperture. The solid line is the function defined by (18) and the dashed line corresponds to the sigmoidal fit given in [1].

where the values of the Jacobi elliptic functions can be determined from (12) and using the identity $\mathrm{sn}^2(u\,|\,m)+\mathrm{cn}^2(u\,|\,m)=1$. After some algebra, we obtain

$$\frac{x_0-a}{b}=\frac{2K}{\pi}\sqrt{\frac{E/K-m_1}{K/E-1}}, \tag{18}$$

where the parameter m of the complete elliptic integrals has once again been suppressed. Equation (18) is plotted in fig. 4 along with the corresponding values computed in [1]. The deviation of (18) from the computed values for the intercept of the ideal aperture are shown (as a fraction of the computed value) in fig. 5.

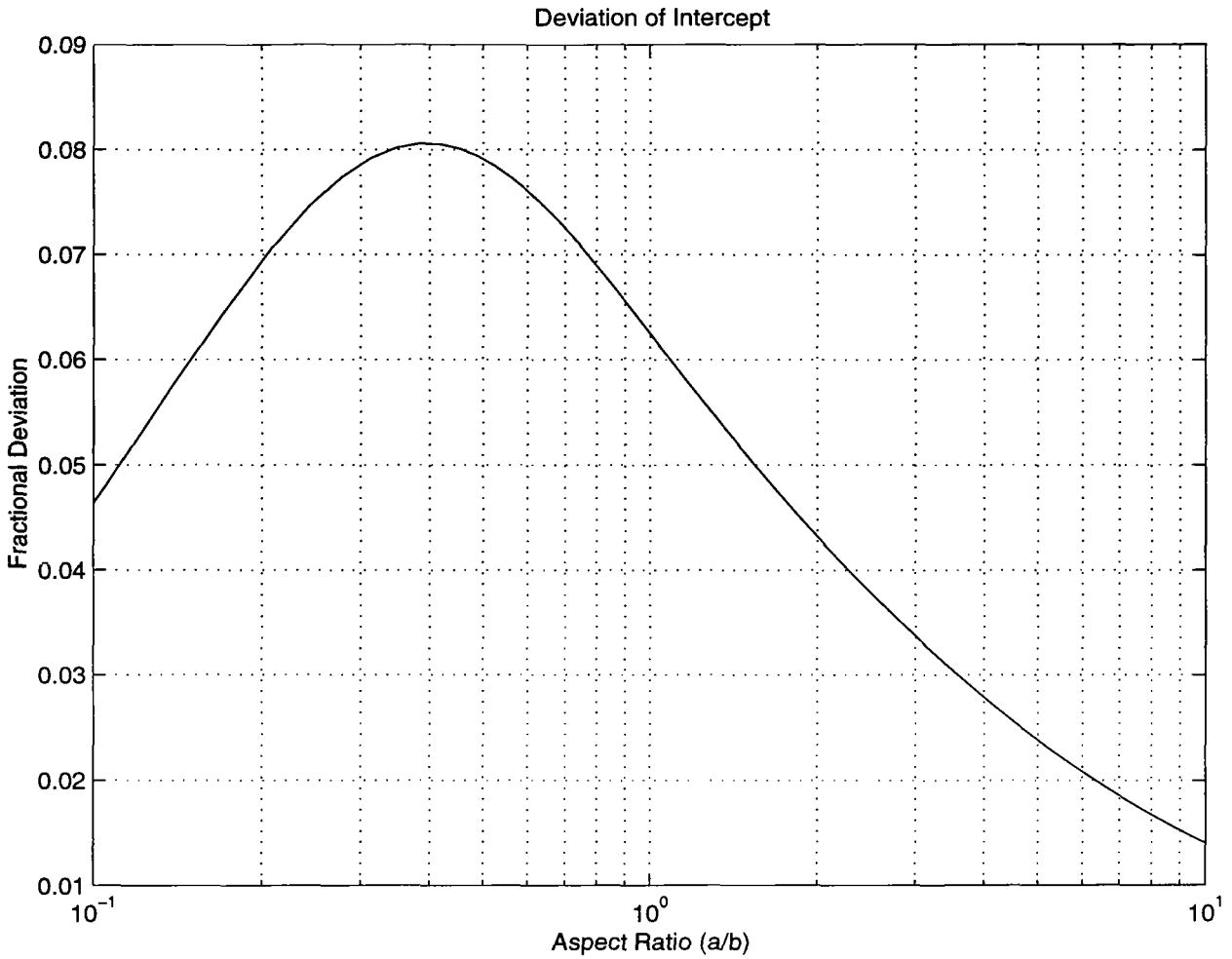

Figure 5: Deviation of the intercept locations shown in fig. 4. Note that the maximum deviation is found for a/b values of just less than 1. Again, this corresponds to the area where the approximation is the poorest, yet, as shown in fig. 6, even the poorest approximation to the aperture boundary is still very close to the computed curve.

C. Similarity of Field Line to Ideal Aperture

In this final section, the contour given by (12) is directly compared to the contours calculated in [1] for several specific aspect ratios. We see that the agreement is very close, and that the aperture given by the field line $u = u_0$ closely approximates the ideal aperture. Figure 6 shows the ideal apertures computed in [1] and the aperture given by the field line that satisfies (12) for several values of the line impedance.

In all cases, as is shown in the plot in fig. 4, the curve obtained by the method described here lies *outside* the ideal aperture calculated in [1]. The additional area does result in a lower efficiency, however, in the four cases presented in fig. 6, the aperture efficiency obtained using the methods presented in this paper were less than 0.5% lower than the efficiency of the of the corresponding ideal aperture. It is thus clear that the analytic methods introduced here provide a good approximation for the ideal aperture.

V. Conclusion

Together with [1], this paper provides a thorough understanding of the concept of aperture efficiency and the properties of the ideal aperture for a flat plate feed structure (as might be found in a lens IRA). As has been shown, the prompt efficiency depends on the choice of the focused aperture, and an optimum aperture does exist. While it is not trivial to find the optimum aperture, the methods introduced here provide a straightforward analytic means to approximate this optimum aperture.

In many (if not most) applications, it is impractical to use the ideal aperture. Due to factors such as ease of manufacture and array packing density, it is often simpler, cheaper, and more effective to use a slightly suboptimal aperture (as was discussed for rectangular and hexagonal packing in [1]). However, the fact that an optimum aperture does exist is important, and should prove helpful when designing an IRA aperture for a particular application.

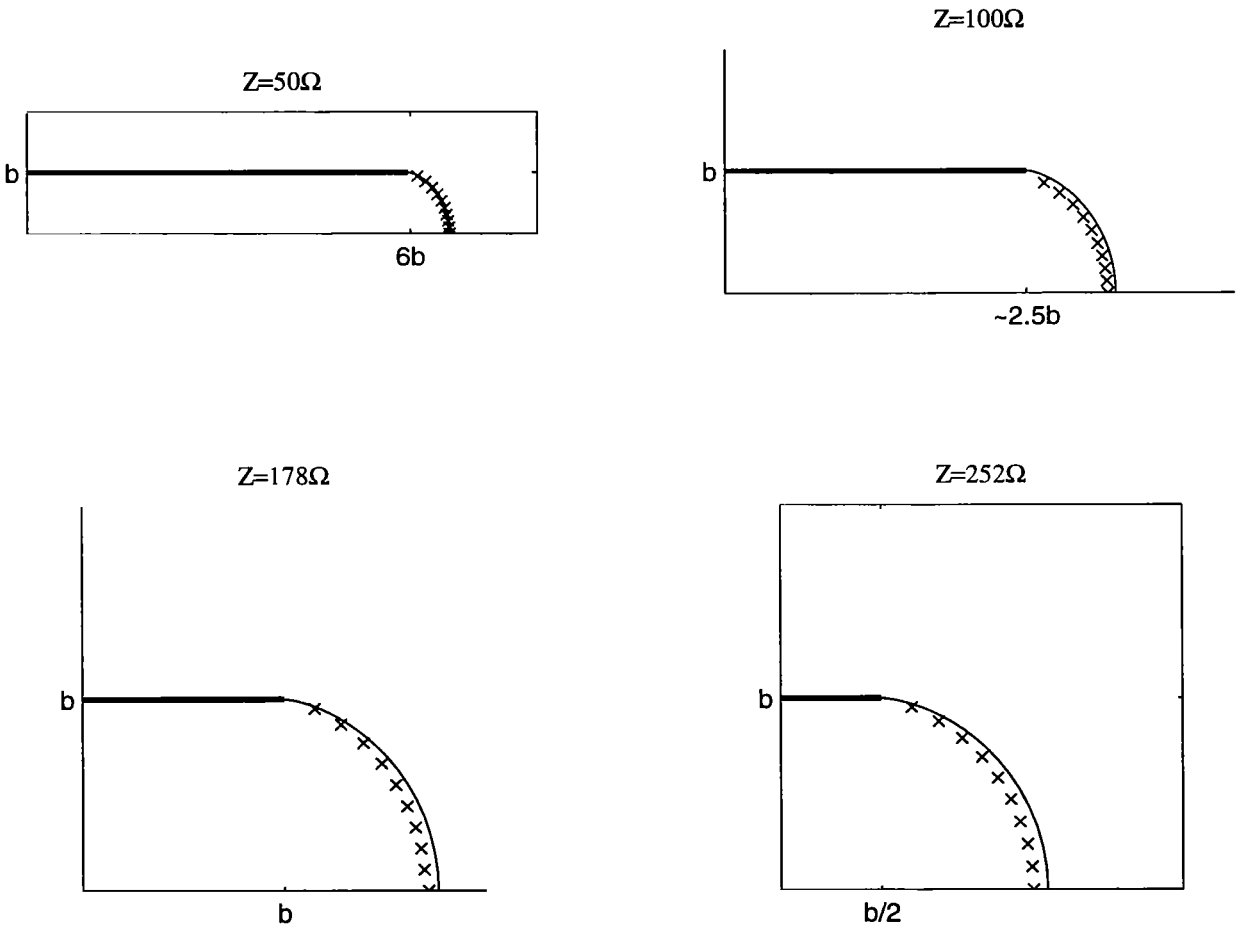

Figure 6: Apertures computed using analytic methods for several line impedances. Points on the ideal aperture, calculated in [1] are also shown. Note that the approximate aperture is in all cases *bigger* than the actual ideal aperture, but a comparison between the efficiencies shows a decrease of less than 0.5%. The Efficiencies of these apertures are all strictly *greater* than that of the corresponding optimum hexagonal and rectangular apertures computed in [1].

REFERENCES:

1. C. J. Buchenauer, J. S. Tyo, and J. S. H. Schoenberg, "Aperture Efficiencies of Impulse Radiating Antennas" *Sensor and Simulation Notes* Note 421, November 1997

2. C. E. Baum, "Radiation of Impulse-Like Transient Fields" *Sensor and Simulation Notes* Note 321, November 1989.

3. P. Moon and D. E. Spencer, *Field Theory Handbook*, Springer-Verlag, Berlin, 1961.

4. W. R. Smythe, *Static and Dynamic Electricity, 3rd Edition*, Taylor and Francis, 1989

5. E. G. Farr and C. E. Baum, "Radiation from Self-Reciprocal Apertures" in *Electromagnetic Symmetry*, C. E. Baum and H. N. Kritikos, Eds. Taylor and Francis, 1995

6. C. E. Baum, "Impedances and Field Distributions for Parallel Plate Transmission Line Simulators" *Sensor and Simulation Notes* Note 21, June 1966

7. C. E. Baum, D. V. Giri, and R. D. Gonzalez, "Electromagnetic Field Distribution of the TEM Mode in a Symmetrical Two-Parallel-Plate Transmission Line" *Sensor and Simulation Notes* Note 219

8. F. C. Yang and K. S. H. Lee, "Impedance of a Two-Conical-Plate Transmission Line" *Sensor and Simulation Notes* Note 221, November 1976

9. E. G. Farr and C. E. Baum, "Impulse Radiating Antennas, Part III" in *Ultra Wideband, Short-Pulse Electromagnetics 3*, C. E. Baum, L. Carin, and A. P. Stone, Eds. Pp. 43-56 (Plenum, New York, 1997)

10. C. J. Buchenauer, J. S. Tyo, and J. S. H. Schoenberg, "Antennas and Electric Field Sensors for Ultra-Wideband Transient Time-Domain Measurements: Applications and Methods" in *Ultra-Wideband, Short-Pulse Electromagnetics 3* C. E. Baum, L. Carin, and A. P. Stone, Eds. pp. 405-422 (Plenum, New York, 1997)

11. M. Abramowitz and I. A. Stegun, *Handbook of Mathematical Functions* (Dover, New York, 1970)